JOURNAL OF SPACECRAFT AND ROCKETS
Vol. 36, No. 4, July–August 1999

Aeroelastic Effects on the Roll Characteristics of a Wraparound Fin Projectile

Seung-Kil Paek* and In Lee†
Korea Advanced Institute of Science and Technology, Taejon 305-701, Republic of Korea

The roll characteristics of a projectile with wraparound fins in the supersonic flow region are analyzed considering the flexibility of the fins. Because of the inherent spin, wraparound fins are subjected to both aerodynamic and centrifugal forces. The aerodynamic force is computed by solving the Euler equations in a body-fixed rotating coordinate frame. A finite element structure modeling and static deflection calculations, resulting from the centrifugal force and the aerodynamic force of the wraparound fin, have been made. The equilibrium spin rate, defined as the spin rate for which the net roll moment is zero, is selected as the major aeroelastic roll parameter. The equilibrium spin rates at various velocity indices and mass ratios are computed. As velocity index or dynamic pressure increases, the equilibrium spin rate increases. The increase of mass ratio or fin mass increases the stiffness of the fin and decreases the effect of aerodynamic force on the equilibrium spin rate.

Nomenclature

A_{ref} = reference area, $\pi D^2/4$, m^2
C_l = roll moment coefficient, $L/\frac{1}{2}\rho_\infty U_\infty^2 A_{\text{ref}}$
C_{l_0} = roll-producing moment coefficient
C_{l_δ} = roll-producing moment coefficient derivative, $\partial C_l/\partial\delta$, per rad
$C_{l_{\Omega^*}}$ = roll-damping moment coefficient derivative, $\partial C_l/\partial\Omega^*$, per rad
D = reference length, the diameter of the projectile body, m
E = Young's modulus, Pa
$\hat{E}, \hat{F}, \hat{G}$ = contravariant flux vectors in generalized coordinates
e = total energy, nondimensionalized by U_∞^2
h = enthalpy, nondimensionalized by U_∞^2
J = flux Jacobian
$K(\Omega)$ = stiffness matrix considering stress stiffening and spin softening due to centrifugal load
$\bar{K}(\bar{\Omega})$ = nondimensionalized stiffness matrix considering stress stiffening and spin softening due to centrifugal load
L = roll moment, N-m
M_0 = reference mass, defined as $\rho_s D^3$, kg
M_∞ = freestream Mach number
$\boldsymbol{P}_a$ = aerodynamic force vector
$\boldsymbol{P}_c$ = centrifugal force vector
$\bar{\boldsymbol{P}}_c$ = centrifugal force vector, nondimensionalized by $M_0 D\omega_0^2$
p = pressure, nondimensionalized by $\rho_\infty U_\infty^2$
p_∞ = freestream static pressure, Pa
$\hat{\boldsymbol{Q}}$ = conservative flow variable vector
$\hat{\boldsymbol{S}}$ = source vector due to rotating coordinate frame
U, V, W = contravariant velocities along the generalized coordinates
U_∞ = freestream flow speed, m/s
u, v, w = Cartesian velocities component, nondimensionalized by U_∞
u_0 = fin deflection, m
$\bar{u}_0$ = nondimensionalized fin deflection, nondimensionalized by D
V_I = velocity index, defined as $U_\infty/\omega_0 D\sqrt{\mu}$
x, y, z = Cartesian coordinates, nondimensionalized by D
γ = specific heat ratio
μ = mass ratio, defined as $2M_0/\rho_\infty D^3$
ξ, η, ζ = generalized coordinates
ρ = air mass density, nondimensionalized by ρ_∞
ρ_s = structural mass density
ρ_∞ = freestream air mass density, kg/m^3
Ω = roll spin rate, rad/s
$\bar{\Omega}$ = structural spin parameter, roll spin rate nondimensionalized by ω_0
Ω^* = roll spin rate, nondimensionalized by U_∞/D
Ω^*_{eq} = equilibrium roll spin rate, nondimensionalized by U_∞/D
ω_0 = reference frequency, defined as $\sqrt{(ED/M_0)}$, rad/s

Introduction

WRAPAROUND fins, which are curved in the spanwise direction, have been used primarily for their advantages in packaging tube-launched projectiles during the past few decades. These surfaces can fold against the cylindrical projectile body and be made to fit into a launch tube, allowing more efficient use of space. Thus, a greater number of wraparound fin projectiles can be stored in the same space as fixed-fin projectiles designed to deliver the same payload. Because of their special geometric shape, these wraparound fins produce roll moment even at zero angle of attack, which results in a spin in which the roll direction changes as the Mach number varies.[1]

The accurate prediction of the roll characteristics of projectiles is important in projectile designs. As the rotation of the projectile about the body axis at a low spin rate can minimize the effect of aerodynamic and inertial asymmetries on the free-flight trajectory, conventional projectiles as well as wraparound fin projectiles have proper spin rates. A good design will require an equilibrium spin rate that avoids both the (rigid body) yawing frequency and the projectile's first natural frequency of vibration. The yawing frequency is avoided to preclude the possibility of spin/yaw lock in, which may lead to increase in yaw during flight. If the flight body experiences spin rates near the first natural frequency of vibration, severe bending of the body may occur. Typically, the first natural frequency and the yawing frequency represent an upper and lower bound of the design equilibrium spin rate.[2]

Because of high dynamic pressure in low altitude where the projectiles mainly operate, the roll characteristics of projectiles with flexible fins are expected to be different from those with rigid fins. Because of spanwise curvature, spinning wraparound fins are subjected to the bending moments caused by the centrifugal forces. Hence, the wraparound fins are affected by centrifugal forces as well as aerodynamic forces. These roll characteristics will vary depending on how flexible the structure is. The current concern is the

Received 23 December 1997; revision received 5 January 1999; accepted for publication 29 January 1999.

*Graduate Research Assistant, Department of Aerospace Engineering.
†Professor, Department of Aerospace Engineering. Senior Member AIAA.

aeroelastic effects on the roll characteristics of wraparound fins in the supersonic range. In this paper a numerical study was conducted for a wraparound fin with double-wedge cross section. This is the first known research about the aeroelastic roll characteristics of the wraparound fin.

The roll behavior of a flight vehicle can be characterized by the roll-producing moment coefficient, the roll-damping moment coefficient, and the equilibrium spin rate. The roll-producing moment coefficient is defined as the roll moment coefficient produced in the absence of spin. The roll-damping moment coefficient is defined as the roll moment coefficient derivative with respect to nondimensionalized spin rate. The equilibrium spin rate is defined as the spin rate at which the net roll moment is zero. Although the prediction of the roll-producing moment is conceptually straightforward, the roll-damping moment requires predictions of the roll moment in the presence of spin. The steady flowfield about a body in rolling motion can be observed from a body-fixed coordinate frame.[3] A body-fixed rotating coordinate frame is used in the current study to predict the roll characteristics for a wraparound fin projectile at zero angle of attack.

Analyses on roll characteristics of even rigid wraparound fins are rare. Only the roll-producing moment coefficient had been determined for nonaxisymmetric bodies using Euler or Navier–Stokes computational methods.[4–6] Projectile designers relied on approximate methods[7] to determine the roll-damping moment coefficient or the steady-state spin rate. Recently, Weinacht and Sturek[8] applied a computational method based on parabolized Navier–Stokes equations to determine the roll-producing moment coefficient, the roll-damping moment coefficient, and the equilibrium spin rate of a nonaxisymmetric body.

In this paper the aerodynamic force is computed by solving the Euler equations. The governing equations are appropriately modified to include the Coriolis and centrifugal accelerations resulting from the rotating coordinate frame. A finite element modeling of the fin structure and the static deflection computation by the centrifugal force and the aerodynamic force of the wraparound fin have been made by the multipurpose finite element code EMRC/NISA.[9] The EMRC/NISA code can consider the centrifugal force resulting from the fin mass itself as a body force and stress stiffening and spin softening effects. Considering the computed structural deflection, the aerodynamic mesh is updated, and the aerodynamic force is recalculated. The procedure is repeated to obtain a converged solution.

For a consistent analysis a nondimensionalized aeroelastic equation was formulated considering the spinning motion. Nondimensionalized aeroelastic parameters, such as velocity index and mass ratio, were devised. For various velocity indices and mass ratios the aeroelastic effects on the equilibrium roll rate of a projectile with wraparound fins are studied.

Aerodynamic Model

The Euler equations of a strong conservative form in a generalized coordinate system are given as[10]

$$\frac{\partial \hat{\boldsymbol{Q}}}{\partial \tau}+\frac{\partial \hat{\boldsymbol{F}}}{\partial \xi}+\frac{\partial \hat{\boldsymbol{G}}}{\partial \eta}+\frac{\partial \hat{\boldsymbol{H}}}{\partial \zeta}=\hat{\boldsymbol{S}} \tag{1}$$

where the conservative variable vector $\hat{\boldsymbol{Q}}$, the flux vectors $\hat{\boldsymbol{F}}$, $\hat{\boldsymbol{G}}$, and $\hat{\boldsymbol{H}}$, and the source vector $\hat{\boldsymbol{S}}$ are

$$\hat{\boldsymbol{Q}}=J^{-1}[\rho \quad \rho u \quad \rho v \quad \rho w \quad \rho e]^T \tag{2}$$

$$\hat{\boldsymbol{F}}=J^{-1}[\rho U \quad \rho u U+\xi_x p \quad \rho v U+\xi_y p \quad \rho w U+\xi_z p \quad \rho U h+U_\Omega p]^T$$

$$\hat{\boldsymbol{G}}=J^{-1}[\rho V \quad \rho u V+\eta_x p \quad \rho v V+\eta_y p \quad \rho w V+\eta_z p \quad \rho V h+V_\Omega p]^T \tag{3}$$

$$\hat{\boldsymbol{H}}=J^{-1}[\rho W \quad \rho u W+\zeta_x p \quad \rho v W+\zeta_y p \quad \rho w W+\zeta_z p \quad \rho W h+W_\Omega p]^T$$

$$\hat{\boldsymbol{S}}=J^{-1}[0 \quad 0 \quad \Omega^* \rho w \quad -\Omega^* \rho v \quad 0]^T \tag{4}$$

where the rotation axis is the x axis, whose direction is from the projectile nose to the tail, and

$$U=\xi_x u+\xi_y v+\xi_z w-U_\Omega, \qquad V=\eta_x u+\eta_y v+\eta_z w-V_\Omega$$

$$W=\zeta_x u+\zeta_y v+\zeta_z w-W_\Omega \tag{5}$$

$$U_\Omega=\xi_y(-\Omega^* z)+\xi_z(\Omega^* y), \qquad V_\Omega=\eta_y(-\Omega^* z)+\eta_z(\Omega^* y)$$

$$W_\Omega=\zeta_y(-\Omega^* z)+\zeta_z(\Omega^* y) \tag{6}$$

The pressure p and enthalpy h can be related to the dependent variables by applying the ideal gas law:

$$p=\rho(\gamma-1)\left[e-\tfrac{1}{2}(u^2+v^2+w^2)\right] \tag{7}$$

$$h=e+p/\rho \tag{8}$$

For a numerical implementation we used the finite volume method for the spatial discretization and the diagonally approximate factorization method by Pulliam and Chaussee[11] for the time integration. A more detailed explanation about the numerical technique is available in Refs. 4 and 10.

Aeroelastic Equation

A structural equilibrium equation can be written as

$$[K(\Omega)]\{u_0\}=\{P_a\}+\{P_c\} \tag{9}$$

The aerodynamic load vector is changed by the fin deflection and can be written as

$$\{P_a\}=\tfrac{1}{2}\rho_\infty U_\infty^2\{\Delta C_p(u_0,\Omega)A\} \tag{10}$$

where ΔC_p and A are the pressure coefficient difference between the convex side and the concave side of the wing and the area associated with ΔC_p. From Eqs. (9) and (10), the nondimensional equilibrium equation can be written as

$$M_0 D\omega_0^2[\bar{K}(\bar{\Omega})]\{\bar{u}_0\}=\tfrac{1}{2}\rho_\infty U_\infty^2 D^2\left\{\Delta C_p\left(\bar{u}_0,\Omega^*\right)\bar{A}\right\}$$

$$+M_0 D\omega_0^2\{\bar{P}_c(\bar{u}_0,\bar{\Omega})\} \tag{11}$$

Equation (11) can be rewritten in more compact form as

$$[\bar{K}(\bar{\Omega})]\{\bar{u}_0\}=V_I^2\left\{\Delta C_p\left(\bar{u}_0,\Omega^*\right)\bar{A}\right\}+\{\bar{P}_c(\bar{u}_0,\bar{\Omega})\} \tag{12}$$

The nondimensional spin rates $\bar{\Omega}$ and Ω^* are related as

$$\bar{\Omega}=(V_I\sqrt{\mu})\Omega^* \tag{13}$$

The square of the structural spin parameter $\bar{\Omega}^2$ can be considered as the ratio of centrifugal force to structural stiffness or the ratio of inertia force to elastic force by the following relationship:

$$\frac{\Omega^2}{\omega_0^2}=\frac{M_0 D\Omega^2}{M_0\omega_0^2 D}=\frac{M_0 D\Omega^2}{E}$$

The square of velocity index is the ratio of dynamic pressure to structural stiffness or the ratio of aerodynamic force to elastic force by the following relationship:

$$V_I^2=\frac{U_\infty^2}{\omega_0^2 D^2\mu}=\frac{1}{2}\frac{\rho_\infty U_\infty^2 D}{M_0\omega_0^2}=\frac{1}{2}\frac{\rho_\infty U_\infty^2}{E}$$

For the constant E, the square of the velocity index is linearly related to dynamic pressure. Hence, the increase of the velocity index can be thought to be the increase of dynamic pressure. The mass ratio is the ratio of the structural mass density to the air density. The increase in mass ratio can be thought to be the increase of the wraparound fin mass.

Roll Characteristics

In linear roll motion the roll moment is linearly related to fin cant angle δ and roll rate as

$$C_l = C_{l_\delta}\delta + C_{l_{\Omega^*}}\Omega^* \tag{14}$$

However, wraparound fins have nonzero roll moment even without cant angle and roll rate; therefore, Eq. (14) needs to be rewritten as

$$C_l = C_{l_0} + C_{l_\delta}\delta + C_{l_{\Omega^*}}\Omega^* \tag{15}$$

Mikhail[7] has devised a correlation between C_{l_δ} and $C_{l_{\Omega^*}}$ based on the previous experimental data. His correlation for wraparound fins is written as

$$\frac{-2C_{l_{\Omega^*}}}{C_{l_\delta}(y_c/d)(l/h)^m} = 2.15 \tag{16}$$

where y_c is the distance between the body roll axis and the area center of one fin panel and l/h is the ratio of the arc length of the curved fin chord to the distance between the two fin endpoints. The exponent m varies with M_∞ as $0.1(1 + M_\infty + \frac{2}{3}M_\infty^2)$. This correlation will be used for comparison with the roll-damping moment computed by the present Euler code.

Aeroelastic Analysis Procedure

The aeroelastic computation procedure is as follows: For the desired velocity index, mass ratio, and spin rate Ω^*, $\bar{\Omega}$ is computed by Eq. (13) and used as an input to compute centrifugal force. Without aerodynamic force a NISA run is made, and the deflection by centrifugal forces is computed. To consider the stress-stiffening and spin-softening effects caused by the initial centrifugal load, a nonlinear static analysis option is set. To consider the computed structural deflection, the aerodynamic mesh of the fin surface is updated using the surface spline method.[12] The aerodynamic grid points in the inner domain are updated by spring analogy method.[13] The aerodynamic load for the updated aerodynamic grid at a spin rate ratio Ω^* is computed and converted to finite element method (FEM) nodal forces by the surface spline method. Another NISA run is made. The following relaxation is introduced to reduce the computational oscillations:

$$\{\bar{u}_0\}^{n+1} = \{\bar{u}_0\}^n + \theta\left(\{\bar{u}_0\} - \{\bar{u}_0\}^n\right) \tag{17}$$

where $\bar{u}_0$ is the deflection on a wing surface mesh point, $\bar{u}_0^n$ is the deflection at the nth iteration, and θ is a relaxation factor and is selected between 0.7 and 0.85. The entire procedure is repeated to obtain a converged solution. The realistic magnitude of the fin deflection can be obtained by multiplying $\bar{u}_0$ by D. The preceding procedure is not for dynamic aeroelastic analyses, such as flutter, but only for static analyses.

Euler Code Validation

Two configurational models were used in this analysis. The first model was used to compare the roll-producing moment coefficients computed by the present aerodynamic code with the experiment. The second model was used to compare the computed roll-damping moment coefficients with a correlation[6] based on experiment data and was used for the aeroelastic analysis. As a basic configuration, a standard wraparound fin projectile determined by the TTCP (Technical Cooperation Program),[1,6,14] as shown in Fig. 1, was used. The body-fixed coordinate system and positive roll direction are also shown in Fig. 1. The first model is the same as the standard TTCP configuration, which had fins with symmetric leading- and trailing-edge bevels. The detailed fin geometry is shown in Fig. 2. The second model has fins with wing-tip bevel (Fig. 3). The second model will

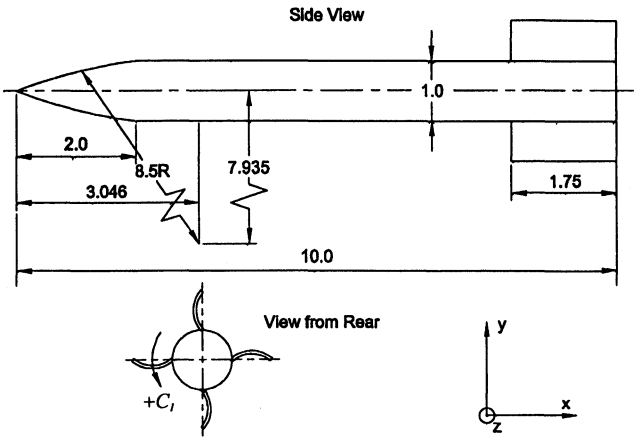

Fig. 1 Geometry of the TTCP standard projectile (in calibers).

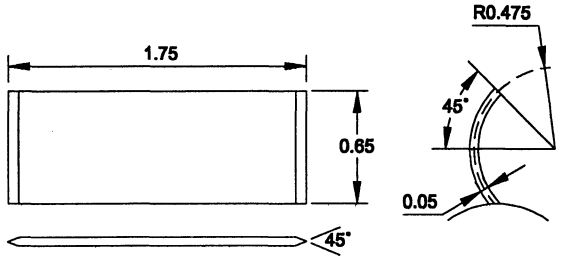

Fig. 2 Fin shape of the TTCP standard model (in calibers).

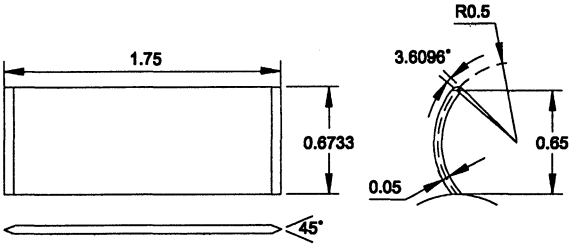

Fig. 3 Fin shape used for computational model (in calibers).

be denoted as the aeroelastic model. The domain of calculation was taken to be the region between the two fins with the upper surface (concave side) of one fin and the lower surface (convex side) of the adjacent fin as the boundaries of the domain. This region is referred to here as a fin passage. In general, to model the influence of adjacent fins, the entire projectile with all of the fins needs to be solved. However, for the axisymmetric flowfield with zero angle of attack considered here, all fin passages can be assumed to be identical, and only one fin passage needs to be solved by enforcing the conditions of symmetry. The experimental data for the TTCP standard model used for comparison were obtained from Ref. 6 and are originated in Ref. 14. The experimental data themselves were made from the flight test at the Jet Propulsion Laboratory (JPL). Figure 4 is a graph showing the variations of roll moment coefficient with Mach number for the computations made by using the present Euler code and the experimental data obtained at JPL. The positive roll is defined in Fig. 1. Figure 4 shows that the roll moment coefficients computed with the present Euler code agree well with the trend and the magnitude of the experimentally obtained data. Another result by Edge[6] is that for the fin with the same configuration except the blunt leading and trailing edge. See Ref. 4 for a detailed description and discussion about this result.

As already mentioned, wraparound fins undergo spin by the roll moment generated because of the spanwise curvature. From roll moment values computed at several selected roll rates, an equilibrium roll rate can be determined easily for the rigid wing. This computational procedure is demonstrated in Fig. 5, which is a plot for the roll rate-roll moment coefficient curves of the aeroelastic model at $M = 1.3$, 1.7, 2.2, and 2.6. At $M = 1.3$ and 1.7, the equilibrium roll

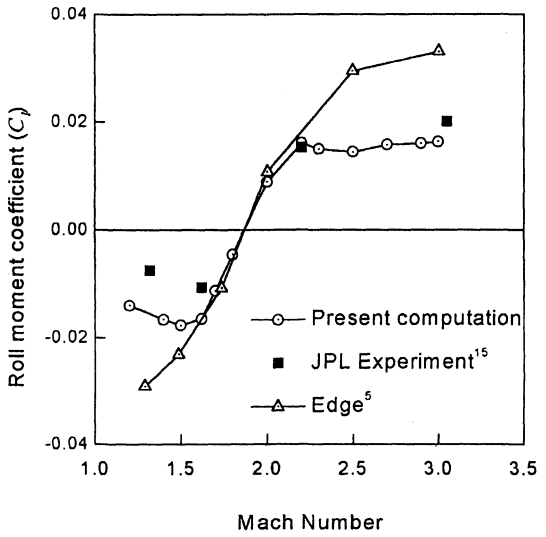

Fig. 4 Roll moment coefficient vs Mach number for computational and JPL experimental data.

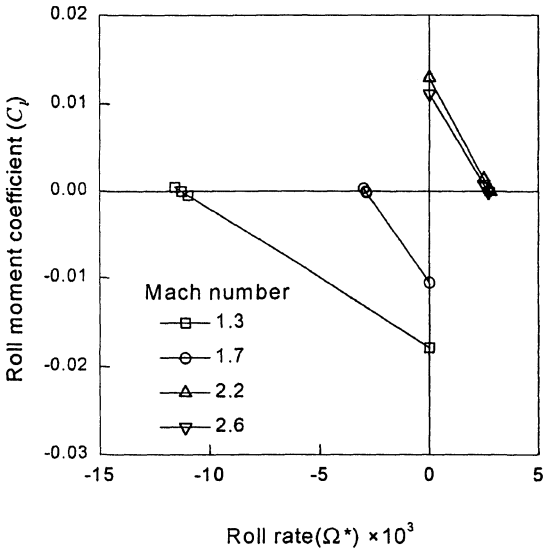

Fig. 5 Roll moment coefficient vs roll rate at various Mach numbers (for rigid fin).

rates are negative, and at $M = 2.2$ and 2.6, they are positive. The roll moment coefficients change as a linear function of the roll rate. This trend is the same as that for a nonaxisymmetric projectile found in the reference of Weinacht and Sturek.[7] The equilibrium roll rates at various Mach numbers for the aeroelastic model are shown in Fig. 6. We can see that the roll reversal point, defined as the Mach number at which the roll direction changes, is at about $M = 1.8$. The grid system used for the aeroelastic model is H–H type and its dimension is 85 × 25 × 41 (Ref. 10). The roll-damping coefficients for the rigid fin are computed from the roll rate–roll moment coefficient curves at various Mach numbers. The roll-damping coefficients for wraparound fins are said to be difficult to obtain even experimentally, and experimental data for comparison are rare. Hence, they are compared with those computed by Mikhail's correlation of Eq. (16) (Table 1 and Fig. 7). C_{l_δ} for the wraparound fin is needed to make use of Mikhail's correlation and is obtained by comparing the roll moment coefficient at cant angles $\delta = -0.5$ deg and that without cant, as shown in Table 1. The correlation gives a somewhat larger value in magnitude than the present computation, but the computed values agree well with the trend and the magnitude. As the correlation for wraparound fins is based on only one experimental data set,[7] the authors do not think that the present comparison is sufficient evidence for the accuracy of the computation but do think that the present computer code gives satisfactory results.

Table 1 Mikhail's correlation values at various Mach numbers

M	$C_{l_{\Omega^*}}$	C_{l_0}	C_l^a	$C_{l_\delta}^b$	$2C_{l_{\Omega^*}}/C_{l_\delta}(y_c/d)^c[(l/h)^d]^m$
1.3	−1.585	−0.01789	−0.03593	2.067	1.77492
1.5	−2.404	−0.02045	−0.04926	3.301	1.67727
1.8	−4.125	−0.00082	−0.04606	5.184	1.81694
2.0	−4.451	0.00873	−0.03759	5.308	1.90203
2.15	−4.625	0.01352	−0.03581	5.653	1.84595
2.5	−4.277	0.01072	−0.03806	5.590	1.70361
2.7	−4.317	0.01167	−0.03489	5.336	1.78659

[a]Roll moment coefficient at cant angle $\delta = -0.5$ deg. [b]$[(C_l^a - C_{l_0})/(-0.5 \times \pi/180)]$. [c]$(y_c/d) = 0.8366$. [d]$(l/h) = 1.0972$.

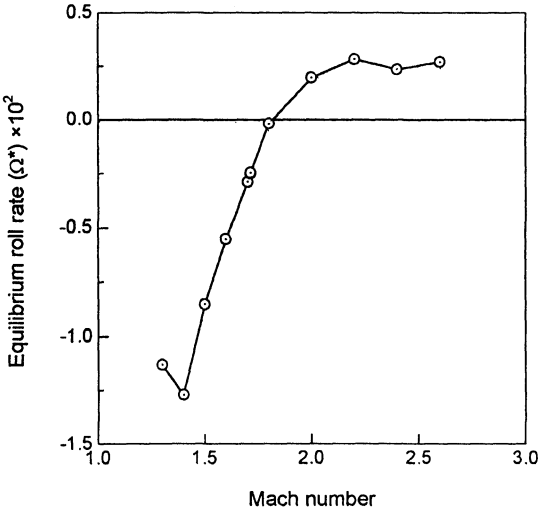

Fig. 6 Equilibrium roll rates at various Mach numbers.

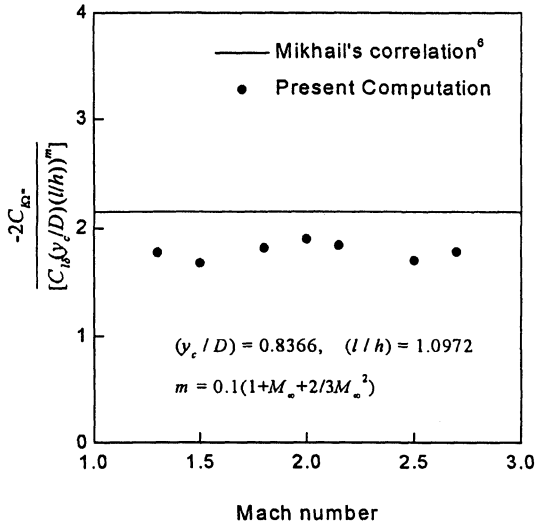

Fig. 7 Roll-damping moment coefficients at various Mach numbers.

Aeroelastic Analysis

The fin structure is modeled using 4 × 8 eight-node quadrilateral general shell elements in the EMRC/NISA code. The number of the finite elements are sufficient for the present analyses. To choose appropriate values for the nondimensional parameters, the material properties for 6061-T6 aluminum alloy and the aerodynamic properties for the sea-level standard atmosphere are used. The data set used is listed in Table 2. The velocity index changes as a function of Mach number. Velocity indices at two Mach numbers are given in Table 3 for the assumed speed of sound. The order of the velocity indices is about 10^{-3} and that of the mass ratios is about 10^3. For the velocity index range from 0 to 3.0×10^{-2} and the mass ratio range from 10^2 to 10^5, the aeroelastic equilibrium roll rates were

Table 2 Structural and aerodynamic properties used for the selection of the aeroelastic parameters

Property	Value
Structural[a]	
Young's modulus, E	70 Gpa
Shear modulus, G	29 Gpa
Mass density, ρ_s	2860 kg/m^3
Aerodynamic[b]	
Speed of sound, a	340.3 m/s
Air density	1.225 kg/m^3

[a]The material properties of 6061-T6 aluminum alloy.
[b]The aerodynamic properties at sea level.

Table 3 Parameters computed using the properties of Table 2

Parameter	Value
D	0.1016 m
M_0	3.000 kg
ω_0	48694 rad/s
μ	4669.4
V_I	1.2079×10^{-3}[a]
	$\sim 2.6172 \times 10^{-3}$[b]

[a]The value determined at $M = 1.2$.
[b]The value determined at $M = 2.6$.

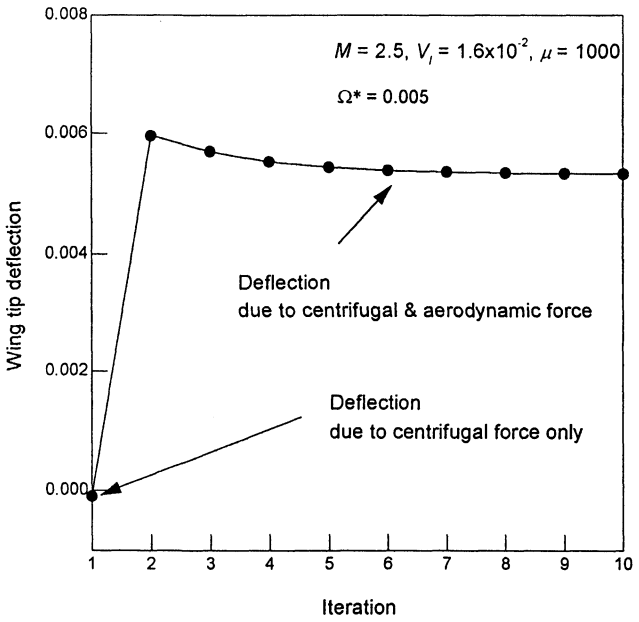

Fig. 8 Convergence history of static deflection at the trailing edge of the fin tip.

computed. The selected nondimensional parameters are somewhat greater than the realistic value in magnitude but are used to observe more clearly the aeroelastic effects. The analysis has been done at $M = 1.714$ and 2.5. The equilibrium roll rates for the rigid wing at both Mach numbers are the same in magnitude but are different in sign ($\Omega^*_{eq} = 2.51 \times 10^{-3}$). In other words, comparing the aeroelastic equilibrium roll rates at the Mach numbers where the magnitudes of equilibrium roll rates for rigid wing are the same, the change of aeroelastic effects with respect to Mach number are observed.

Figure 8 shows a typical convergence history of the static deflection for a parameter set where $M = 2.5$, $V_I = 1.6 \times 10^{-2}$, $\mu = 1000$, and $\Omega^* = 0.005$. It is a plot of the static deflection in the y-axis direction at the trailing edge of the fin tip. In Fig. 8, the static deflection caused by the centrifugal force is small compared with the static deflection caused by the aerodynamic force because of small $\bar{\Omega}(= 0.0025)$. From the computations performed in this analysis, the

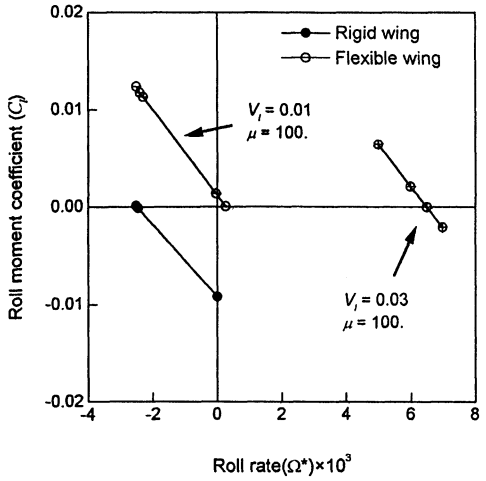

Fig. 9 Comparison between roll moment coefficient curves of rigid and flexible wraparound fin at $M = 1.714$.

static wing-tip deflections at $\bar{\Omega} = 0.02$ and 0.04 are calculated to be -0.004 and -0.014, respectively. For the converged static deflection and flowfield, the roll moment coefficient is computed. Figure 9 shows the variations of the roll moment coefficient with the roll rate for the elastic wing as well as for the rigid wing at $M = 1.714$. The roll moment coefficient of the flexible wing changes as a linear function of roll rate, as well as that of the rigid one. From Fig. 9 we can observe that the roll-producing moment coefficient, the equilibrium roll rate, and the roll-damping moment coefficient of the elastic wing increase as the velocity index increases.

Figures 10a and 11a show the aeroelastic equilibrium roll rates computed at various velocity indices and mass ratios at $M = 1.714$ and 2.5. From those figures one can see that the equilibrium roll rate increases as the velocity index increases. Figure 12 shows the pressure distribution and static deflection along the chord at the 96% arc length of the leading edge at the equilibrium roll rate for the case that $M = 2.5$, $V_I = 3.2 \times 10^{-2}$, and $\mu = 1000$. The pressure difference between the convex and concave side of the wrap-around fin acts as a nose-down moment. As the increase in the velocity index means the increase in the dynamic pressure, it gives an increase in the leading-edge deflection, the local angle of attack, and the roll-producing moment. Hence, the increase in the velocity index increases the equilibrium roll rate. The preceding results are therefore reasonable. Moreover, the roll reversal point can be changed because of aeroelastic effect.

Figures 10a and 11a also show that at a larger mass ratio the change of equilibrium roll rate with velocity index is smaller, which means that the aeroelastic effect decreases as the mass ratio increases. As the change of the equilibrium roll rate is much smaller than the change of the mass ratio, the increase in mass ratio is directly related to the increase of $\bar{\Omega}$ as seen in Figs. 10b and 11b. As already seen, increasing $\bar{\Omega}$ means increasing centrifugal force. Centrifugal force may increase the stiffness of the wraparound fin because of the combined effect of stress stiffening and spin softening. Hence, one can think that increasing the mass ratio increases the stiffness of the wraparound fin and decreases the effect of the aerodynamic force represented by the velocity index, which explains Figs. 10a and 11a.

At $M = 1.714$, incidentally, the rigid wing spins in the negative direction, but the roll direction of the flexible wing changes as the velocity index increases (see Fig. 10a). At $M = 2.5$ the trend is the same as that at the lower Mach number, but the change of the equilibrium roll rate with the increasing velocity index is smaller (Fig. 11a).

The aspect ratio, or the ratio of span to fin chord of the computational model used in this paper, is much smaller than that of the other wraparound fin projectiles.[1,7] The thought is that the aeroelastic effects of the larger aspect ratio wraparound fins will become larger than the present model because their torsional stiffness will be smaller.

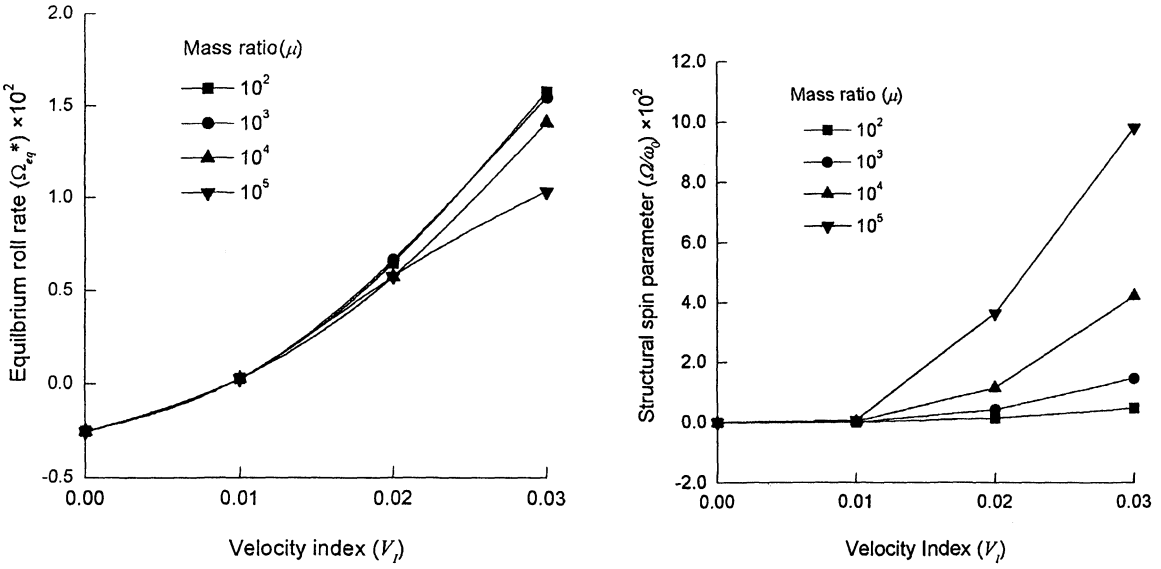

a) Velocity index vs equilibrium roll rate

b) Mass ratio vs structural roll parameter

Fig. 10 Aeroelastic equilibrium roll rate at M = 1.714.

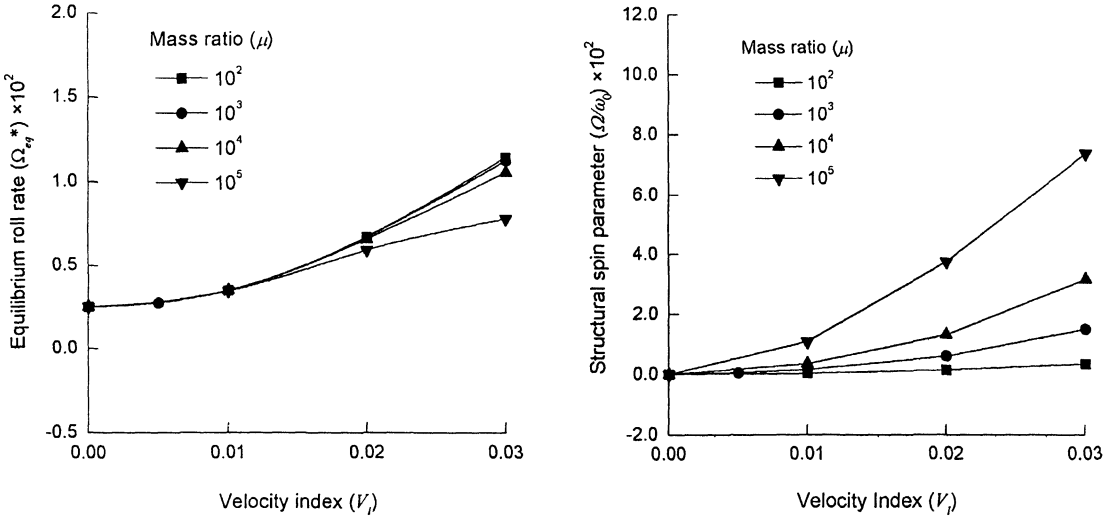

a) Velocity index vs equilibrium roll rate

b) Mass ratio vs structural roll parameter

Fig. 11 Aeroelastic equilibrium roll rate at M = 2.5.

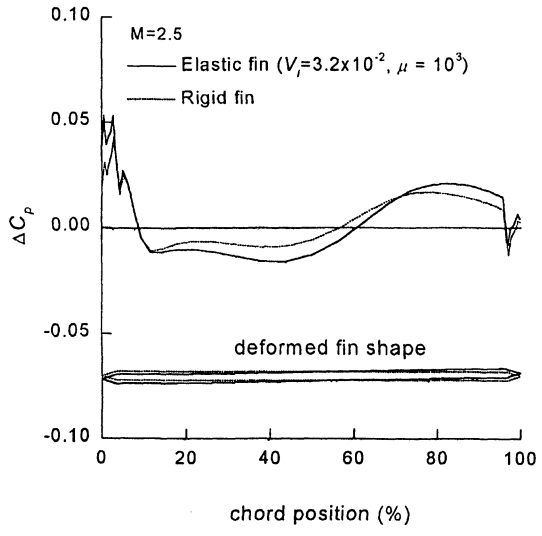

Fig. 12 Pressure distribution at the 96% arc length along the leading edge of the wraparound fin at the equilibrium roll rate.

Conclusions

The aeroelastic roll characteristics for a projectile with wraparound fins are computed in the supersonic regime. This is the first research about the aeroelastic roll characteristics of the wraparound fin. The flowfield is computed by solving the Euler equation in a body-fixed rotating coordinate frame. From the computed flowfield the aerodynamic roll parameters are determined. The predictions of the roll-producing and roll-damping moment coefficients for the rigid fin have been compared with experimental data and with results obtained using a correlation based on previous experiment data, respectively.

A finite element structure modeling and static deflection computation of the elastic wraparound fins, resulting from the centrifugal force and the aerodynamic load, have been made by the EMRC/NISA code. The equilibrium spin rates of a projectile with the elastic fin at various velocity indices and mass ratios have been determined. From these results the following conclusions are obtained.

The increase in velocity index (or dynamic pressure) increases the equilibrium roll rate. In other words, the effect of aerodynamic force for flexible wraparound fins is to increase the equilibrium roll rates. Hence, the roll reversal point can be changed. This indicates that aeroelastic effect can be an important factor in the roll characteristics

of the wraparound fin. Increasing mass ratio decreases the effect of velocity index on equilibrium spin rate. In other words, the increase in mass ratio (or wraparound fin mass) increases the stiffness of the fin and decreases the effect of aerodynamic force on the equilibrium spin rate. As already noted, the first natural frequency of the flexible projectile and the (rigid body) yawing frequency represent an upper and lower bound of the design equilibrium spin rate. As the aeroelastic effects increase the spin rate, the thought is that the design equilibrium spin rate may as well exist near the lower bound. When an excessive increase of the spin rate is anticipated, the designer may as well consider a mass distribution to increase the centrifugal force.

The aspect ratio of the computational model used in this study is much smaller than the conventional wraparound fin projectile,[1,7] for which the aeroelastic effects may become larger. Subsequent studies for larger aspect ratio fins are anticipated.

Acknowledgment

The work presented in this paper was supported by the Agency for Defense Development in Korea. This support is gratefully acknowledged.

References

[1]Winchenbach, G. L., Buff, R. S., Whyte, R. H., and Hathaway, W. H., "Subsonic and Transonic Aerodynamics of a Wraparound Fin Configuration," *Journal of Guidance, Control, and Dynamics*, Vol. 9, No. 6, 1986, pp. 627–632.

[2]Baines, D. J., and Pearson, K. G., "Aeroelasticity as a Consideration in Aerodynamic Design of Rolling, Unguided Research," *Journal of Aircraft*, Vol. 4, No. 12, 1967, pp. 1603–1608.

[3]Schiff, L. B., "Nonlinear Aerodynamics of Bodies in Coning Motion," *AIAA Journal*, Vol. 10, No. 11, 1972, pp. 1517–1522.

[4]Paek, S. K., Park, T.-S., Bae, J.-S., Lee, I., and Kwon, J. H., "Computation of Roll Moment for Projectile with Wraparound Fins Using Euler Equation," *Journal of Spacecraft and Rockets*, Vol. 36, No. 1, 1999, pp. 53–58.

[5]Wardlaw, A. B., Priolo, F. J., and Solomon, J. M, "Multiple-Zone Strategy for Supersonic Missiles," *Journal of Spacecraft and Rockets*, Vol. 24, No. 4, 1987, pp. 377–384.

[6]Edge, H. L., "Computation of the Roll Moment for a Projectile with Wrap-Around Fins," *Journal of Spacecraft and Rockets*, Vol. 31, No. 4, 1994, pp. 615–620.

[7]Mikhail, A. G., "Roll Damping for Projectiles Including Wraparound, Offset, and Arbitrary Number of Fins," *Journal of Spacecraft and Rockets*, Vol. 32, No. 6, 1995, pp. 929–937.

[8]Weinacht, P., and Sturek, W., "Computation of the Roll Characteristics of a Finned Projectile," *Journal of Spacecraft and Rockets*, Vol. 33, No. 6, 1996, pp. 769–775.

[9]*NISA II USER'S MANUAL*, Ver. 6.0, Engineering Mechanics Research Corp., Troy, MI, 1996.

[10]Paek, S. K., and Lee, I., "Static Aeroelastic Analysis for Wrap-Around Fins of a Rolling Projectile," *Proceedings of JSASS 11th International Sessions in 35th Aircraft Symposium*, 1997, pp. 647–650.

[11]Pulliam, T. H., and Chaussee, D. S., "A Diagonal Form of an Implicit Approximate Factorization Algorithm," *Journal of Computational Physics*, Vol. 39, No. 2, 1981, pp. 347–363.

[12]Harder, R. L., and Desmarais, R. N., "Interpolation Using Surface Spline," *Journal of Aircraft*, Vol. 9, No. 2, 1972, pp. 189–191.

[13]Robinson, B. A., Batina, J. T., and Yang, H. T. Y., "Aeroelastic Analysis of Wings Using the Euler Equations with a Deforming Mesh," AIAA Paper 90-1032, April 1990.

[14]Dahlke, C. W., "The Aerodynamic Characteristics of Wrap-Around Fins at Mach Numbers of 0.3 to 3.0," U.S. Army Missile Command, TR RD-77-4, Redstone Arsenal, AL, Oct. 1976.

R. M. Cummings
Associate Editor